High-Order Harmonic Transient Grating Spectroscopy in a Molecular Jet

Y. Mairesse,[1,2] D. Zeidler,[1,3] N. Dudovich,[1,4] M. Spanner,[5] J. Levesque,[1] D. M. Villeneuve,[1] and P. B. Corkum[1]

[1]*National Research Council of Canada, 100 Sussex Drive, Ottawa, Ontario K1A 0R6, Canada*

[2]*Centre Lasers Intenses et Applications, Université Bordeaux I, UMR 5107 (CNRS, Bordeaux 1, CEA), 351 Cours de la Libération, 33405 Talence Cedex, France*

[3]*Carl Zeiss SMT AG, D-73447 Oberkochen, Germany*

[4]*Department of Physics of Complex Systems, Weizmann Institute of Science, Rehovot 76100, Israel*

[5]*Chemical Physics Theory Group, Department of Chemistry, and Center for Quantum Information and Quantum Control, University of Toronto, Toronto, M5S 3H6 Canada*

(Received 11 May 2007; revised manuscript received 2 October 2007; published 11 April 2008)

We study high-order harmonic generation in excited media using a four-wave-mixing-like configuration. We analyze the spatial profile of high harmonics emitted by a grating of rotationally excited molecules as a function of the pump-probe delay. We demonstrate a dramatic improvement in the contrast of the diffracted signal relative to the total high harmonic signal. This allows us to observe subtle effects in the rotational wave packet excitation such as the pump-intensity dependence of the wave packet dynamics. High harmonic transient grating spectroscopy can be extended to all forms of molecular excitation and to weak resonant excitation.

DOI: 10.1103/PhysRevLett.100.143903 PACS numbers: 42.65.Ky, 33.15.Mt, 33.80.Rv

Transient grating spectroscopy (TGS) is the method of choice for measuring femtosecond dynamics in solids, liquids, or gases whenever background suppression is important [1,2]. In TGS, temporal information about the low-order nonlinear light-matter interaction is mapped into the spatial domain where it can be observed against a zero background. Thus, TGS allows measurements where only a small fraction of the molecules are excited, as the diffracted signal only arises from exactly this fraction.

If we could extend TGS from perturbative nonlinear optics to nonperturbative nonlinear optics, then it could be applied in high harmonic generation (HHG) experiments. This would be important since the harmonic signal encodes structural information on the orbital which can be used to perform a full reconstruction of an orbital [3]. It would benefit any measurement where a modification of the orbital, resulting from a rotational [4–6], vibrational [7–9], electronic [10,11], or photochemical excitation, is measured.

We show that TGS can be applied where the probe pulse is intense enough to create high harmonics or attosecond pulses. We use two beams to create a grating of molecular excitation and a third beam to generate high-order harmonic radiation. The pump and probe beams do not temporally overlap, and the excitation and harmonic generation processes are thus decoupled. We study the case of rotational wave packets in N_2 molecules because their behavior is so well understood that we are able to critically examine the applicability of strong field TGS. We compare the total harmonic signal with the transient grating signal measured from the far-field spatial profile. We obtain a contrast enhancement from the transient grating signal with respect to the total signal that reaches 300:1. Our sensitivity allows us to observe that the second order diffraction peak revives at a different time than the first order peak and that the full and half revivals are not exactly time reversed. These are two subtle effects of strongly excited rotational wave packets.

Transient grating spectroscopy is a special case of nonlinear space-time coupling. It will be clear from our results that space-time coupling can be used in strong field and attosecond science, in much the same way that it is used in perturbative nonlinear optics.

Rotational wave packets can be created in molecules by focusing an intense laser pulse in a gas jet [12,13]. A superposition of rotational states is then excited, leading to the appearance of a periodic structure in the dynamics of the molecular alignment distribution. The periodicity of these revivals is equal to the rotational period of the considered molecule. Many studies of the rotational wave packet dynamics have been carried out, showing that molecules are aligned parallel to the pump laser polarization slightly after the revival time and antialigned (i.e., contained in a plane perpendicular to the pump polarization) slightly before [14]. Around the half-revival time, a similar (but reversed) evolution exists: molecules are first aligned, then antialigned. In addition to this transient alignment evolution, a permanent ''incoherent alignment'' is created by the pump pulse: the alignment distribution is slightly peaked along the laser polarization even off the revivals [14].

Since HHG results from the interference of an electron wave packet driven by the laser field and the molecular orbital [15,16], it is sensitive to the alignment of the molecule with respect to the laser polarization. Several experimental studies of the harmonic emission in rotationally excited molecules have revealed different behaviors for different molecular species [4,5]. We focus on N_2, for

 © 2008 The American Physical Society

which the harmonic emission is maximum when molecules are aligned parallel to the generating laser polarization.

Our experimental setup is presented in Fig. 1. The incoming laser pulse is first split in two by a polarizer associated with a half-wave plate. This allows balancing the relative intensities of the transmitted and reflected beams. The reflected beam polarization is rotated by a half-wave plate, and the beam is split in two by a 50:50 beam splitter. The two parts are vertically shifted in the two arms of the delay line. At the exit of this setup, we obtain three parallel beams with horizontal polarization. The three pulses are focused by a 50 cm lens below a pulsed gas jet with 3 atm backing pressure and a nozzle diameter of 250 μm. The medium length is estimated to 1 mm and the gas density is 10^{17} cm^{-3}.

The central beam generates high harmonics. Its waist at focus is $\sim$100 μm and the intensity is $\sim 1.5 \times 10^{14}$ W cm^{-2}. The harmonic signal is measured by a spectrometer made of a concave grating with variable groove spacing that images the spectrum in the horizontal plane while letting the beam diverge in the vertical plane. The spectrally resolved far-field harmonic profiles are detected by microchannel plates and a charge-coupled device camera.

The two outer beams are the pump beams. They are separated by 30 mm before the lens and arrive Δt before the generating pulse. They interfere at the focus, creating horizontal planes of bright and dark pump intensity separated by $\delta = 13.3$ μm. The pump beam waist at focus is $w_0^{\text{pump}} \approx 150$ μm, and we use peak intensity I^{pump} (at the maximum of the interference fringes) between 4×10^{13} and 2×10^{14} W cm^{-2}. The molecular excitation is spatially modulated by the interference fringes. In the regions of maximum pump intensity, a rotational wave packet is created. The molecular alignment distribution in these planes will evolve as discussed previously, with revivals of alignment and antialignment. By contrast, in the planes of zero pump intensity the alignment distribution remains isotropic.

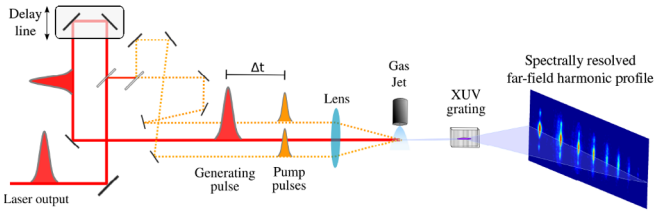

FIG. 1 (color online). Experimental setup. A grating of molecular excitation is created by the two synchronized outer laser pulses. The delayed central pulse generates high harmonics in the excited medium. The harmonics are spectrally resolved in the horizontal plane by an extreme UV spectrometer and spatially resolved in the vertical plane. The image shown in the figure was obtained in N_2 at $\Delta t = 4.0$ ps and corresponds to harmonics 17 to 31, from left to right. Diffraction peaks are visible up and down the harmonics.

Figure 2(a) presents the far-field profiles of harmonic 17 obtained in N_2 with $I^{\text{pump}} = 4 \times 10^{13}$ W cm^{-2}, at two different pump-probe delays. The dashed line is the profile obtained at $\Delta t = 3.5$ ps. Calculations show that at this delay, the molecular alignment distribution is almost isotropic (the degree of alignment is $\langle \cos^2\theta \rangle = 0.35$ while it is 0.33 in the isotropic case). When the delay is set to $\Delta t = 4.0$ ps, which corresponds to the maximum alignment of the molecules, the total harmonic signal is stronger [Fig. 2(b)]. In that case we observe a diffraction peak on each side of the harmonic profile [Fig. 2(a)]. The peaks are centered on ± 3.5 mrad, which corresponds to a near field interfringe of 13.5 μm, in good agreement with the excitation beam's separation. The diffraction efficiency, defined as the fraction of the total signal that appears in a single diffracted order, is 8%.

We have studied the behavior of harmonic 17 as a function of the pump-probe delay [Figs. 2(b) and 2(c)], around the first half and full revival of N_2. The dotted curve presents the evolution of the total signal, normalized to its maximum value. It is increased by a factor of 2 between $\Delta t = 3.5$ and $\Delta t = 4.0$ ps (alignment). At $\Delta t = 4.4$ ps, there is a minimum which corresponds to the antialignment of the molecules. We observe the time-reversed shape around the full revival [Fig. 2(c)].

The evolution of the diffracted light is also presented in Figs. 2(b) and 2(c) (solid line). It is obtained by the selection of one of the diffraction peaks observed in Fig. 2(a). A strong signal is detected at the alignment revivals ($\Delta t = 4.0$ and 8.6 ps). The ratio between the signal off and on the revivals is 60. The contrast in the detection of the alignment revival is thus increased by a factor of 30 by the implementation of a grating of excitation. The diffracted signal presents a secondary maximum when molecules are antialigned ($\Delta t = 4.4$ and 8.2 ps). The diffraction efficiency is then weaker than at alignment (4%).

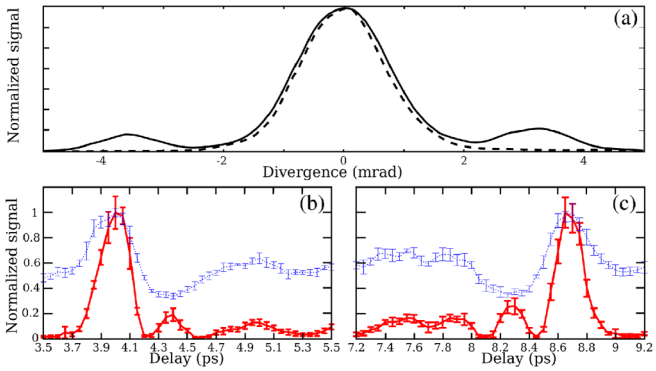

FIG. 2 (color online). (a) Far-field spatial profiles of harmonic 17 generated in N_2 by a grating of rotationally excited molecules, off (dashed line, $\Delta t = 3.5$ ps) and on (solid line, $\Delta t = 4.0$ ps) the half revival of molecular alignment. (b–c) Evolution of the harmonic 17 total signal (dotted line) and diffracted signal (solid line) as the pump-probe delay is scanned over the half (b) and full (c) revival of N_2, with $I^{\text{pump}} = 4 \times 10^{13}$ W cm^{-2}.

In conventional studies of high harmonic emission by rotationally excited molecules, the pump intensity is limited to the threshold intensity of harmonic generation. In our case, however, any harmonic radiation generated by the pump pulses is not detected because it is emitted in other directions. The pump pulses can also create an electron grating. However, this grating is permanent on the time scale probed in the experiment, and therefore, its contribution is similar to that of permanent alignment. The pump intensity is ultimately limited by the buildup of free electrons that can induce phase mismatch and reduce the harmonic signal. Experimentally, this occurs when $I^{\text{pump}} > 2 \times 10^{14}$ W cm^{-2}.

The pump-probe scan for $I^{\text{pump}} = 1 \times 10^{14}$ W cm^{-2} is presented in Fig. 3(a). The delay is scanned over two complete revivals. The total signal is modulated around half and quarter revivals. We have calculated the corresponding evolution of the rotational wave packet with the method detailed in [14] [Fig. 3(b)], with a rotational temperature of 30 K. At this pump intensity, the degree of incoherent alignment is $\langle \cos^2\theta \rangle = 0.4$. As a result, the baseline of the total signal increases by a factor of 1.3 as the delay passes through zero.

The contrast of the grating is set by the difference between the isotropic distribution and the alignment in the excited regions [gray area in Fig. 3(b)]. The incoherent alignment creates a permanent grating in the medium, which produces diffracted light: the permanently diffracted light (baseline of the diffracted signal for positive delays) is 5 times higher than the background signal (measured at negative delays).

The diffracted signal presents peaks every time the contrast of the grating goes through a maximum. This is the case when $\langle \cos^2\theta \rangle$ is maximum, around full, half, and quarter revivals. The contrast in the detection of the revivals of alignment is here 300:1.

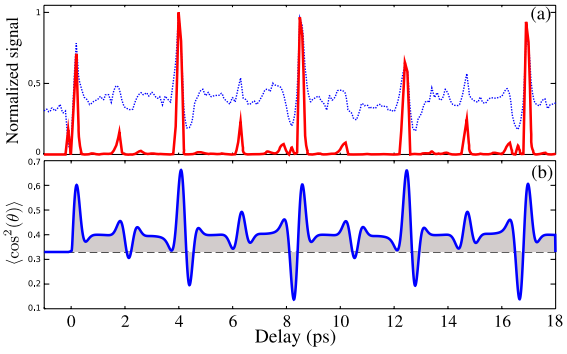

FIG. 3 (color online). (a) Evolution of the harmonic 17 total signal (dotted line) and diffracted signal (solid line) as the pump-probe delay is scanned over the first two revivals of N_2 with $I^{\text{pump}} = 1 \times 10^{14}$ W cm^{-2}. (b) Calculated evolution of the molecular alignment distribution under the same conditions. The dashed line corresponds to an isotropic distribution ($\langle \cos^2\theta \rangle = 0.33$). The gray area represents the contrast of the alignment grating.

The diffracted signal corresponding to antialignment is very weak, especially around the half revivals ($\Delta t = 4.3$ and $\Delta t = 12.8$ ps). We observe a systematic decrease of the diffracted light at $\Delta t = 4.3$ ps as the pump intensity increases. This is due to the increase of the baseline of the alignment distribution, which lowers the contrast of the grating at antialignment. In fact, this effect has recently been studied by four-wave mixing TGS of rotational wave packets at high pump intensity [17]. It results from the interference of the light diffracted by the permanent incoherent grating and the transient grating. This heterodyning leads in general to an increase of the diffracted light at alignment and a decrease at antialignment [17,18]. Around full revivals ($\Delta t = 8.2$ and $\Delta t = 16.6$ ps), the antialignment is more pronounced and the contrast of the grating is higher, leading to a significant diffraction. The difference between half and full revivals, which is clear on the simulations, is hard to distinguish on the total harmonic signal but is revealed by high harmonic TGS. The fact that we are able to detect such subtle structures shows that the very high sensitivity of TGS can be transferred from low-order to high-order nonlinear optics. In the following we increase the pump intensity even further and show that high harmonic TGS can map the intensity dependence of the rotational wave packet dynamics.

The dynamics of the rotational wave packet depends on its bandwidth, i.e., on the number of rotational levels that are coherently coupled by the pump pulse. As the pump intensity increases, this bandwidth increases and the alignment distribution evolves faster around revivals [14]. All pump intensities are present across each grating period. Therefore, wave packets with different bandwidths are excited across each grating line. The simulated temporal evolution of the alignment distribution in the grating of rotational excitation at $I^{\text{pump}} = 2 \times 10^{14}$ is shown in Fig. 4(a). As expected, the evolution is not uniform. The alignment is maximized earlier in the regions of lower

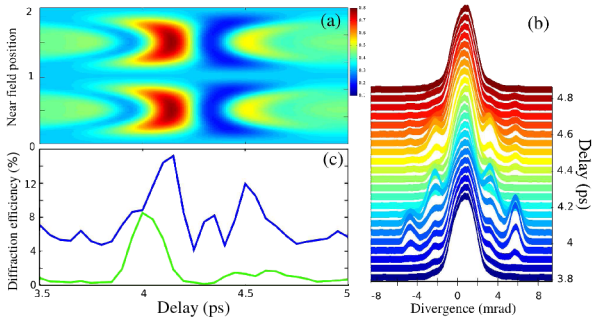

FIG. 4 (color online). (a) Simulated evolution of the molecular alignment distribution $\langle \cos^2\theta \rangle$ in the generating medium as a function of delay, in N_2 at $I^{\text{pump}} = 2 \times 10^{14}$ W cm^{-2}. The vertical axis is in units of the IR grating periodicty. The IR intensity is maximum in 0.5 and 1.5. (b) Measured harmonic 17 spatial profile as a function of pump-probe delay in the same conditions. (c) Measured first order (top line) and second order (bottom line) diffraction efficiency as a function of delay.

intensity. Since the structure of each grating line is time dependent, the diffraction pattern must also be time dependent.

Figure 4(b) presents the evolution of the measured harmonic 17 spatial profile as a function of pump-probe delay at $I^{\text{pump}} = 2 \times 10^{14}$. Around $\Delta t = 4$ ps we observe a first and second order diffraction peak on each side of the central lobe. The evolution of the diffraction efficiency for the two orders is shown in Fig. 4(c). The diffraction efficiency is very high: it reaches about 13.5% for the first order and 8% for the second order.

The first and second order peaks do not pass through their maximum at the same delay. Their different behavior is caused by the anharmonicities of the grating. As predicted [Fig. 4(a)], at $\Delta t = 4.1$ ps the regions of maximum alignment are located where $I = 2 \times 10^{14}$ W cm^{-2}, i.e., on the maxima of the IR interference fringes. At $\Delta t = 4.0$ ps, they are located where $I = 1 \times 10^{14}$ W cm^{-2}, which means that there are two regions of maximum alignment in each fringe of the IR interference pattern. This doubles the periodicity of the diffraction grating [Fig. 4(a)] and leads to the appearance of second order diffracted peaks [Fig. 4(c)].

In conclusion, we have transposed the concept of transient grating spectroscopy from perturbative nonlinear optics to high-order harmonic generation. This has allowed us to increase the contrast for detecting revivals of molecular alignment from 2:1 to 300:1. The high contrast allows us to observe two subtle rotational wave packet effects that are not visible by Coulomb explosion imaging [14] or in the high harmonic spectrum [4,5]. First, we have measured a difference between the time-reversed half revival and the full revival in N_2. Second, we have measured different temporal evolutions for the first and second order diffraction peaks caused by the multiphoton nature of rotational wave packet excitation.

The diffraction pattern measured in our experiment results from the interference of multiple harmonic sources with different alignments and is therefore sensitive to both amplitude and phase modulations. In that sense, TGS can be considered as a special case of high harmonic electron interferometry [19]. The diffraction efficiency can be used to extract the phase modulation induced by the grating.

The high contrast of TGS is well suited to reconstructing the molecular orbital [3] in weakly excited media. High harmonic TGS will be applied to a broad range of time-resolved measurements of electronic, vibrational, rotational, or photochemical excitations [7–9,11]. A first experiment could be the time-resolved observation of a molecular orbital during the dissociation of a diatomic molecule.

Finally, we address the potential for extending measurements to the short pulse limit. It is important because it will be difficult to efficiently optically excite attosecond electron wave packets—both the transition moments and the sources are weak. In the configuration that we presented, propagation of the pump pulse across the probe volume imposes a limit to the temporal resolution that can be achieved. However, transient grating spectroscopy is a special case of space-time coupling. Many configurations offer contrast enhancement without degrading the time resolution. If the pump pulse copropagates along the path of the probe pulse, but with a smaller beam diameter, then the excitation dynamics that it creates forms a transient lens. Now the dynamics is impressed on the far-field beam profile of the attosecond pulse as a function of its delay. There is no degradation of the temporal resolution in this configuration. Similarly, if the pump pulse copropagates but overlaps only one side of the probe volume, then the excitation wave packet forms a transient wedge that can deflect the far-field pattern of an attosecond pulse. Again, there is no degradation of the temporal resolution. For the foreseeable future, space-time coupling will be important for experiments on photo-excited attosecond electron wave packet dynamics.

We thank Kevin Lee for fruitful discussions. We acknowledge partial financial support from the National Research Council of Canada, the Alexander von Humboldt Foundation, the Canadian Institute for Photonic Innovation, the NSERC Accelerator grant program, and the NSERC Special Research Opportunities grant program.

[1] M. D. Levenson, *Introduction to Nonlinear Laser Spectroscopy* (Academic, New York, 1982).
[2] S. Mukamel, *Principles of Nonlinear Optical Spectroscopy* (Oxford University, New York, 1995).
[3] J. Itatani *et al.*, Nature (London) **432**, 867 (2004).
[4] T. Kanai, S. Minemoto, and H. Sakai, Nature (London) **435**, 470 (2005).
[5] J. Itatani *et al.*, Phys. Rev. Lett. **94**, 123902 (2005).
[6] C. Vozzi *et al.*, Phys. Rev. Lett. **95**, 153902 (2005).
[7] M. Lein, Phys. Rev. Lett. **94**, 053004 (2005).
[8] N. Wagner *et al.*, Proc. Natl. Acad. Sci. U.S.A. **103**, 13 279 (2006).
[9] S. Baker *et al.*, Science **312**, 424 (2006).
[10] P. M. Paul *et al.*, Phys. Rev. Lett. **94**, 113906 (2005).
[11] H. Niikura, D. M. Villeneuve, and P. B. Corkum, Phys. Rev. Lett. **94**, 083003 (2005).
[12] H. Stapelfeldt and T. Seideman, Rev. Mod. Phys. **75**, 543 (2003).
[13] F. Rosca-Pruna and M. J. J. Vrakking, Phys. Rev. Lett. **87**, 153902 (2001).
[14] P. W. Dooley *et al.*, Phys. Rev. A **68**, 023406 (2003).
[15] P. B. Corkum, Phys. Rev. Lett. **71**, 1994 (1993).
[16] K. J. Schafer, B. Yang, L. F. DiMauro, and K. C. Kulander, Phys. Rev. Lett. **70**, 1599 (1993).
[17] V. G. Stavros, E. Harel, and S. R. Leone, J. Chem. Phys. **122**, 064301 (2005).
[18] A. Rouzee, V. Renard, S. Guerin, O. Faucher, and B. Lavorel, Phys. Rev. A **75**, 013419 (2007).
[19] Y. Mairesse *et al.* (to be published).